CRS-based minimum-aperture time migration – a 2D land data case study

Miriam Spinner and Jürgen Mann, University of Karlsruhe*

SUMMARY

The Common-Reflection-Surface stack provides a set of kinematic wavefield attributes that characterize the reflection events in seismic prestack data. One of their applications is the determination of minimum migration apertures in Kirchhoff migration. So far, CRS-based minimum-aperture migration in the time domain was mainly used to provide more reliable and less noisy amplitudes in the migrated image. In this contribution, we demonstrate the potential of the minimum-aperture approach to improve the overall image quality. The theoretical as well as the practical aspects of the application to real data are discussed. We show the improved imaging of fault structures on a 2D land dataset compared to the results of conventional Kirchhoff migration.

INTRODUCTION

The Common-Reflection-Surface (CRS) stack method (see, e. g. Mann et al., 1999; Jäger et al., 2001) is a highly automated imaging process. It can be seen as a generalization of high-density stacking velocity analysis and incorporates neighboring common-midpoint (CMP) gathers. In contrast to conventional stacking approaches, the CRS stack provides an entire set of stacking parameters, the so-called kinematic wavefield attributes. These attributes locally characterize the reflection events in the prestack data in the vicinity of the respective stationary points. Thus, they can be used for various imaging and inversion purposes.

Jäger (2005) employed the CRS attributes in 2D pre- and poststack Kirchhoff depth migration to estimate the size and location of the minimum migration aperture. His primary aim was to improve the migrated image by reducing migration artifacts and avoiding operator aliasing. In addition, the efficiency of the migration process considerably increased.

Spinner and Mann (2005) transferred the minimum-aperture concept to the time-migrated domain to increase the stability and to decrease the sensitivity to migration velocity model errors. Therefore, the time domain approach yields more reliable amplitudes for AVO/AVA analyses. The presented minimum-aperture migration is based on a straight ray approximation to allow an efficient implementation. However, note that the approach is not restricted to this type of time migration.

A first application of the time domain approach to real data has been presented by Kienast et al. (2007). Here, we will revisit a land data example which has previously been discussed by Jäger (2005) for limited-aperture migration in the depth domain. The subsurface is of moderate complexity and, thus, well-suited for time migration. The primary objective for these data is to enhance the resolution of faults in the time-migrated image.

BASICS OF CRS STACK

The CRS method is based on a second-order approximation of the kinematic reflection response of an arbitrarily curved reflector segment with inhomogeneous overburden. In the 2D case, this approximation can be entirely expressed in terms of three stacking parameters, namely the emergence angle α of the central ray and the radii R_{NIP} and R_{N} of wavefront curvatures of two hypothetical waves, the so-called NIP and normal wave, respectively (Hubral, 1983). The commonly used hyperbolic approximation reads (see, e. g., Schleicher et al., 1993):

$$t_{\mathrm{R}}^2(x_{\mathrm{m}},h) = \left[t_0 + \frac{2\sin\alpha\,(x_{\mathrm{m}}-x_0)}{v_0}\right]^2 + \frac{2t_0\cos^2\alpha}{v_0}\left[\frac{(x_{\mathrm{m}}-x_0)^2}{R_{\mathrm{N}}} + \frac{h^2}{R_{\mathrm{NIP}}}\right]. \qquad (1)$$

It describes the reflection traveltime t_{R} along a paraxial ray characterized by source/receiver midpoint x_{m} and half-offset h in terms of the two-way traveltime t_0 along the central normal ray emerging at x_0, the near-surface velocity v_0, and the wavefield attributes α, R_{NIP}, and R_{N}.

As in conventional stacking velocity analysis, the optimum wavefield attributes for each ZO location $P_0 = (x_0,t_0)$ are determined by coherence analysis in the prestack data. However, this analysis is carried out with a spatial operator in a multi-dimensional parameter domain. This finally yields entire sections of the wavefield attributes α, R_{NIP}, and R_{N}, as well as a coherence section. Details on the geometrical interpretation and the determination of the wavefield attributes can, e. g., be found in Mann et al. (1999) and Jäger et al. (2001).

DETERMINATION OF THE MINIMUM APERTURE

The determination of the minimum migration aperture consists of two tasks: the calculation of the stationary point that defines the center for the migration aperture and of the size of the projected Fresnel zone which determines its horizontal extension. The basic concept has been described in Jäger (2005) and is briefly reviewed here in a slightly different notation.

Stationary point

In Kirchhoff migration, the main contribution to the diffraction stack stems from the region where the reflection event is tangent to the migration operator, the vicinity of the so-called stationary point. In order to determine the location of the stationary point, two local slowness vectors $\mathbf{p}_{\mathrm{D}}$ and $\mathbf{p}_{\mathrm{R}}$ associated with the migration operator and the reflection event, respectively, are introduced. The tangency point is encountered when both vectors coincide. For zero offset, the slowness $\mathbf{p}_{\mathrm{R}}$ can be entirely expressed in terms of the emergence angle α: $p_{\mathrm{R},x} = \sin\alpha/v_0$. Note that for the 2D case, it is sufficient to consider the horizontal slowness, only. For time migration with straight rays as considered here, the migration operator as well as its spatial derivatives like $p_{\mathrm{D},x}$ are given by analytic expressions which allow an efficient implementation. In practice, the modulus of the difference between these two horizontal slownesses is calculated and the location of the minimum is regarded as stationary point P_0 for ZO. A minimum slowness difference threshold is defined to avoid the detection of minima which are not related to actual stationary points. The associated coherence values help to decide whether the point is reliable by applying a further user-given threshold.

The concept of the *Common-Reflection-Point (CRP) trajectory* allows to extrapolate the stationary point to finite offset. This trajectory describes all points in the prestack time domain which are associated with the same reflection point in depth. Höcht et al. (1999) derived a second-order approximation in terms of CRS attributes. Its projection onto the acquisition surface reads:

$$x_{\mathrm{m}}(h) = x_0 + r_{\mathrm{T}}\left(\sqrt{\frac{h^2}{r_{\mathrm{T}}^2}+1}-1\right), \qquad (2a)$$

with

$$r_T = \frac{R_{NIP}}{2\sin\alpha}\,. \tag{2b}$$

This approximation provides an offset-dependent and, thus, more accurate reference for the center of the migration aperture compared to the conventional approach which ignores the deviation between CMP and CRP gathers.

Projected Fresnel zone

The final information relevant for the migration with minimum apertures which can be gained from the attributes is the size of the projected ZO Fresnel zone. In terms of CRS attributes, it can be approximated as (see, e. g., Mann, 2002)

$$\frac{W_F}{2} = |x_m - x_0| = \frac{1}{\cos\alpha}\sqrt{\frac{v_0\,T}{2\left|\frac{1}{R_N} - \frac{1}{R_{NIP}}\right|}}\,, \tag{3}$$

where T denotes some measure of the wavelet length. In general, the Fresnel zone size is expected to vary with offset. Unfortunately, this effect is hard to quantify as the velocity model together with the dip and curvature of the reflector has to be considered. However, forward calculated examples suggest that for moderately curved reflectors, the variation is very small. Due to the approximate nature of the Fresnel zone estimate, the actual aperture is usually increased by about 15 to 20% to ensure that the projected Fresnel zone is fully covered by the aperture. This also accounts for the offset-dependent variation in most cases.

PRACTICAL APPLICATION

Preconditioning of the CRS attributes

In Kirchhoff migration, each point on the output grid is treated independently. In the same way, the location of the stationary point and the size of the projected Fresnel zone is determined for each output location independently. Thus, the method strongly relies on the reliability and smoothness of the kinematic wavefield attributes. By means of the event-consistent smoothing (Mann and Duveneck, 2004), outliers and unphysical fluctuations which would deteriorate the minimum-aperture migration result can be removed beforehand.

In general, the estimation of the emergence angle by means of the CRS stack is expected to be rather stable which, therefore, allows a reliable determination of the stationary point. In contrast, the radius of the normal wave is usually the most unstable attribute. This may lead to unreasonable values for the size of the projected Fresnel zone. The effect on the migrated image is usually rather small, but the amplitudes clearly suffer. If stable attributes for the normal wave are not available, a plane wave approximation can be utilized for the projected Fresnel zone by setting the curvature of the normal wave to zero. However, this approach may lead to an underestimation of the Fresnel zone size for strongly curved reflectors.

Criteria for stationary points

The number of locations for which a stationary point is found in the minimum-aperture approach is controlled by the user-given coherence threshold. Ideally, a reliable stationary point can be detected for each sample on an actual reflection event. In real data applications, this situation is rather unrealistic and stationary points are mostly detected on strong reflection events. Decreasing the coherence threshold increases the number of detected stationary points, but may cause artifacts as unreliable attributes are considered. In practice, an appropriate measure between coverage and reliability of the stationary points has to be found.

Transition from minimum to conventional aperture

As the target area cannot be expected to be completely covered with stationary points, the conventional aperture is utilized at all locations where no stationary point was found to avoid gaps in the migrated image. This proceeding leads to local jumps in the aperture size. However, if the conventional aperture is chosen sufficiently large to cover the size of the projected Fresnel zone, the results from the different aperture definitions differ only with regard to the noise level. Prerequisite is, of course, that the location of the stationary point and the projected Fresnel zone size in the minimum-aperture approach are determined from reliable wavefield attributes.

Ambiguities

A special situation arises if reflection events intersect each other in the unmigrated stacked domain (conflicting dip situation). In principle, this case can be handled in the CRS processing by allowing multiple attribute sets for a given ZO location. However, the identification of conflicting dip situations is rather unstable and strongly depends on the choice of appropriate processing parameters. Therefore, the explicit handling of conflicting dip situations is usually omitted in practical applications. However, in case of successfully detected conflicting dip situations, the multiple attribute sets can be fully exploited by the limited-aperture migration approach: the search for the stationary point is simply performed for all available attribute sets. In general, each attribute set will yield a different stationary point related to different migration output locations.

Similar to the ambiguity in the input domain, we can also encounter an ambiguity in the output domain related to multiple stationary points associated with one migration operator. A similar numerical concept as in the CRS conflicting dip handling can be applied to identify such situations. However, this also immediately implies that the same instability and tendency to introduce artifacts can be expected. Therefore, the current implementation of the limited-aperture migration only considers one stationary point per ZO migration operator.

REAL DATA EXAMPLE

The 2D seismic land dataset used for the case study was acquired by an energy resource company in a fixed-spread geometry. The seismic line had a total length of about 12 km. The utilized source signal was a linear upsweep from 12 to 100 Hz of 10s duration. Shot and receiver spacing are both 50 m and the temporal sampling interval is 2 ms. Standard preprocessing was applied to the field data. As the amplitudes were not preserved during this process, the data is not suited to recover reflection amplitudes. Hence, the subsequent discussion of the results is restricted to kinematic aspects.

CRS stack and model building

The CRS stack was carried out on the preprocessed dataset. Conflicting dip situations were not considered. Due to the high data quality, a stable estimation of all attributes was possible even for weak events. An event-consistent smoothing was applied to remove remaining outliers and to precondition the attribute sections for the following steps. For the determination of the time migration velocity model, the smoothed attributes associated with the reflection events have been extracted and converted to time migration velocities (see Mann, 2002). In a subsequent infill procedure, the migration velocities were inter- and extrapolated using a distance weighted polynomial interpolation. The final velocity model is displayed in Figure 1a), selected common-image gathers are depicted in Figure 1b). The gathers show some residual moveout which is most likely related to the utilized straight ray approximation. Hereby, the ray-bending caused by the strong vertical velocity gradient is not taken into account.

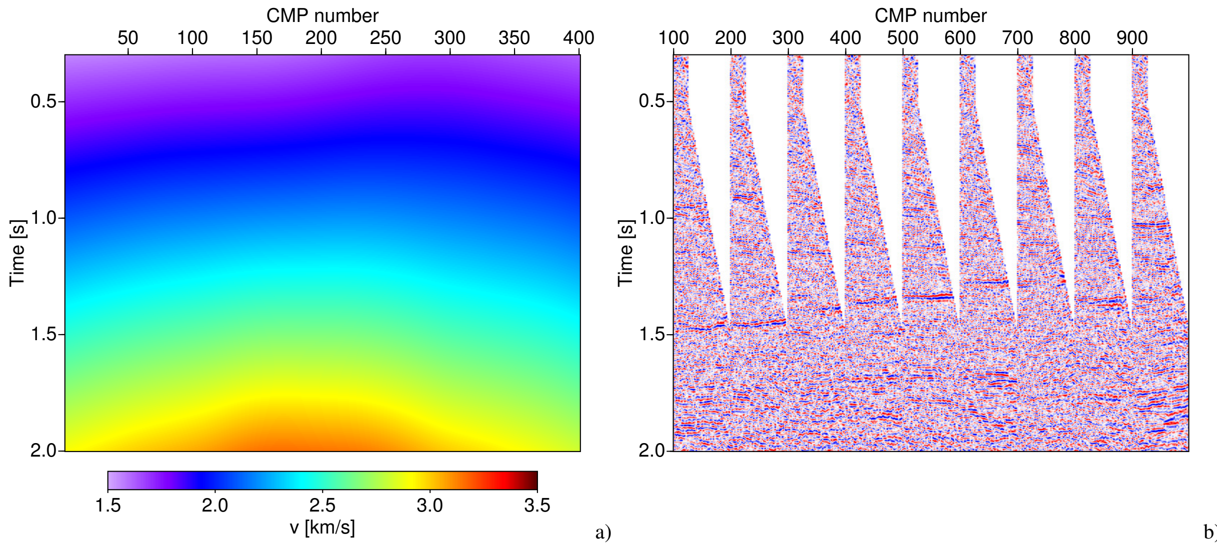

Figure 1: a) Smoothed time migration velocity model derived from the wavefield attributes. b) Selected common-image gathers extracted from the migrated prestack data. The maximum offset is 2000 m. Due to the strong vertical velocity gradient, the employed straight ray approximation leads to some residual moveout.

Poststack migration

The minimum-aperture poststack migration was carried out on the ZO stacked section using the smoothed attribute sections. The determined midpoint displacement of the stationary points with respect to the operator apex for ZO is shown in Figure 2a), the associated half-size of the projected ZO Fresnel zone in Figure 2b). Both attributes are only displayed at locations where stationary points have been detected. For this dataset, a stable determination of stationary points and the corresponding projected Fresnel zone size was possible for nearly the whole target zone. At all other locations, the conventional aperture (described below) was applied to obtain an image without gaps. In correspondence to the subsurface structure, the midpoint displacement increases up to 500 m in the lower part of the dataset where the reflection events become steeper. The Fresnel zone size, which was enlarged by 20% with respect to the values determined from the CRS attributes, increases with increasing traveltime up to 800 m. The high values for the Fresnel zone size determined beyond 1.5 s are related to (fragments of) diffraction events which, theoretically, have an infinite projected Fresnel zone. In conflicting dip situations, only the attribute set associated with the stronger event was available and has been used in the determination of the minimum aperture (see, e. g., the reflection event between CMP 300 and 350 which shows positive midpoint displacement). The migrated section is displayed in Figure 2d).

A second poststack migration was conducted in a conventional way with a user-given aperture centered around the operator apex (Figure 2c)). The aperture linearly increases from 100 m at 0.3 s to 2000 m at 2.0 s. In both conventional and minimum-aperture migration, the same taper has been applied to avoid artifacts related to the boundary of the migration aperture. The minimum-aperture migration result shows a better image quality and more contiguous events compared to the conventionally obtained poststack migration result. The noise level is significantly reduced in all locations where a stationary point could be detected and faults are better defined. The operator aliasing present in the shallow part of the conventional migration result is avoided in the minimum-aperture result as the summation is restricted to the tangency region between migration operator and reflection event. Evidently, the application of an anti-alias filter would clearly improve the conventional result, this, however, influences the migrated amplitudes. Note that the transition between conventional and minimum aperture in Figure 2d) is only characterized by a different noise level.

Prestack migration

In Figure 2e) and Figure 2f), the corresponding prestack migration results are depicted. For both migration approaches, the aperture was kept constant with offset due to the small curvature of the reflection events. Whereas the conventional aperture is still centered around the operator apex for all offsets, the minimum aperture approximately follows the actual stationary point with increasing offset: the CRS-based approximation of the CRP trajectory (equation 2) is used to extrapolate the location of the stationary point to finite offsets starting from the detected location for ZO.

Compared to the poststack results, we observe more detailed subsurface structures but also an increased noise level. The latter is due to the fact that the CRS stacked section used for the poststack migration already has a significantly increased signal-to-noise ratio. Nevertheless, the differences between the conventional and the minimum-aperture migration results shows similar behavior as in the poststack case: a better definition of the faults and more distinctive reflection events in many areas can be seen in the minimum-aperture result. Again, operator aliasing is present in the conventional result. Furthermore, it shows a higher overall noise level.

CONCLUSIONS

The kinematic wavefield attributes obtained by the Common-Reflection-Surface stack method can be employed to estimate minimum apertures for Kirchhoff migration. Concerning dynamic aspects and stability, this approach is particularly suited for time migration. We applied the minimum-aperture approach in the time domain to a 2D land dataset with various fault structures. Similar as shown by Jäger (2005) in the depth domain, the image quality, fault resolution, and the signal-to-noise level in the time-migrated image clearly benefit from this approach. This comes along with an increased computational efficiency due to the reduced number of required summations.

ACKNOWLEDGMENTS

The authors wish to thank the sponsors of the *Wave Inversion Technology* (WIT) Consortium.

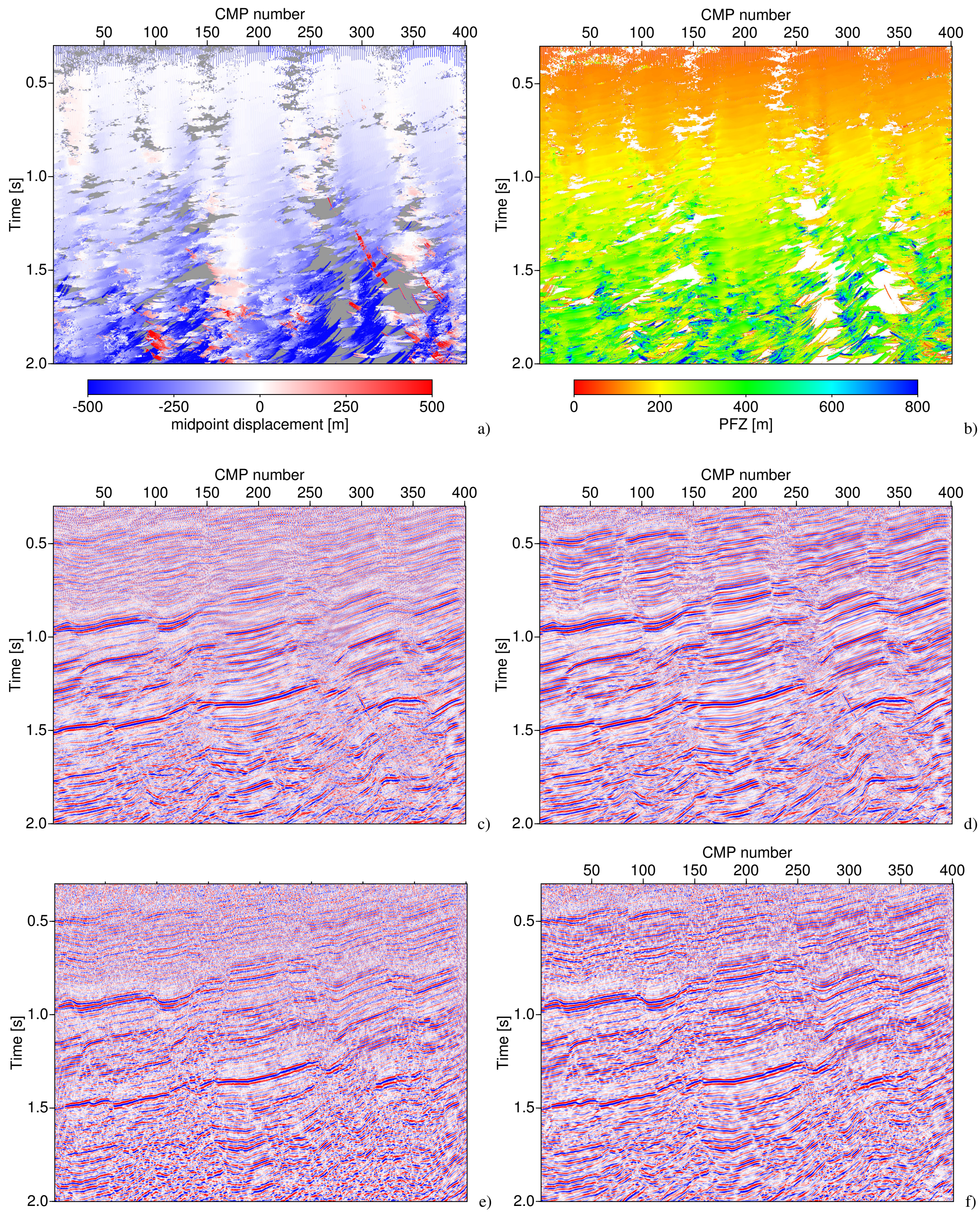

Figure 2: a) Horizontal displacement of the stationary point with respect to the migration operator apex. b) Half-width of the estimated projected Fresnel zone. Due to the high quality of the CRS attributes for these data, stationary points and the corresponding Fresnel zone size could be determined for almost the entire section. Poststack migration results with conventional c) and limited d) aperture. e) and f) The corresponding prestack results after stacking. In the minimum-aperture results, the shallow events are no longer obscured by operator aliasing. The overall image quality has improved and fault locations are better resolved.

REFERENCES

Höcht, G., E. de Bazelaire, P. Majer, and P. Hubral, 1999, Seismics and optics: hyperbolae and curvatures: J. Appl. Geophys., **42**, 261–281.

Hubral, P., 1983, Computing true amplitude reflections in a laterally inhomogeneous earth: Geophysics, **48**, 1051–1062.

Jäger, C., 2005, Minimum-aperture Kirchhoff migration with CRS stack attributes: Logos Verlag.

Jäger, R., J. Mann, G. Höcht, and P. Hubral, 2001, Common-Reflection-Surface stack: image and attributes: Geophysics, **66**, 97–109.

Kienast, M., M. Spinner, and J. Mann, 2007, CRS-based minimum-aperture time migration – a real data example: Presented at the 69th Conf., Eur. Assn. Geosci. Eng. Session P034.

Mann, J., 2002, Extensions and applications of the Common-Reflection-Surface stack method: Logos Verlag.

Mann, J. and E. Duveneck, 2004, Event-consistent smoothing in generalized high-density velocity analysis: Presented at the 74th Ann. Internat. Mtg., Soc. Expl. Geophys. Session ST 1.1.

Mann, J., R. Jäger, T. Müller, G. Höcht, and P. Hubral, 1999, Common-Reflection-Surface stack – a real data example: J. Appl. Geophys., **42**, 301–318.

Schleicher, J., M. Tygel, and P. Hubral, 1993, Parabolic and hyperbolic paraxial two-point traveltimes in 3D media: Geophys. Prosp., **41**, 495–514.

Spinner, M. and J. Mann, 2005, True-amplitude CRS-based Kirchhoff time migration for AVO analysis: Presented at the 75th Ann. Internat. Mtg., Soc. Expl. Geophys. Session AVO 2.4.